Bleustein-Gulyaev waves in a finite piezoelectric material loaded with a viscoelastic fluid

A. El Baroudi[a,*], J. Y Le Pommellec[a]

[a]*LAMPA, Arts et Métiers Sciences et Technologies, 2 bd du Ronceray, 49035 Angers, France*

Abstract

A generalized analytical approach for the propagation of Bleustein-Gulyaev wave in a piezoelectric material loaded on its surface with a viscoelastic fluid is established in this paper. The Bleustein-Gulyaev waveguide surface is subjected to various glycerol concentrations. The Maxwell and Kelvin-Voigt models are used to describe the viscoelasticity of this fluid. Exact dispersion equation is obtained in the cases of both electrically short circuit and open circuit by solving the equilibrium equations of piezoelectric materials and the Stokes equation of viscoelastic fluid. The effect on the phase velocity and attenuation for several frequencies is highlighted. The influence of key parameters such as substrate thickness and fluid thickness is also studied. These investigations can serve as benchmark solution in design of Bleustein-Gulyaev wave sensors.

Keywords: Bleustein-Gulyaev waves, piezoelectric materials, Viscoelastic liquids, Analytical approach.

1. Introduction

Surface acoustic waves sensors have been widely used for sensing applications in both gas and liquid environments. For liquid sensing applications, acoustic waves which have the particle displacement parallel to the device surface and normal to the wave propagation direction are preferred. These waves called shear horizontal waves include Love waves [1, 2, 3, 4, 5, 6] and

*Corresponding author

Email address: adil.elbaroudi@ensam.eu (A. El Baroudi)

Bleustein-Gulyaev waves [7, 8, 9, 10, 11, 12, 13, 14, 15]. The Bleustein-Gulyaev waves have a single component transverse to the propagation direction. The Bleustein-Gulyaev sensor is basically formed by a piezoelectric ceramic covered with a very thin metallic layer [11]. This sensor does not require an aditionnal guiding layer to trap the wave energy to the surface as in the case of the Love Wave sensor [5, 6]. Consequently, the fabrication of the Bleustein-Gulyaev sensors is easier than the contruction of the Love wave sensors. The Bleustein-Gulyaev sensors are used to detect and investigate high pressure phase transitions in food products [16, 17] and Biofuels [18].

The study of the Bleustein-Gulyaev wave interaction with a viscous fluid was conducted [13, 15] by employing the exact theory of continuum mechanics. Nevertheless the exact solution for viscoelastic fluid is still missing. A novel analytical approach of the propagation of Bleustein-Gulaev wave in a piezoelectric material loaded on its surface with a viscoelastic fluid is considered in this paper. The effect of fluid viscoelasticity on the phase attenuation is investigated for several frequencies. The explicit dispersion equations for both open circuit and metallized surface boundary conditions are given. This paper is intended to provide essential data for liquid sensors design and development.

2. Theoretical analysis

2.1. Bleustein-Gulyaev wave

Consider a finite-thickness piezoelectric substrate (ceramic) covered with a finite-thickness layer of viscoelastic fluid, as shown in Figure 1. The Bleustein-Gulyaev wave may exist in piezoelectric materials. It is an electromechanical coupled shear type surface wave, in which the direction of particle motion is perpendicular to the propagating direction and parallel to the surface of piezoelectric substrate. If there is no piezoelectric effect, Bleustein-Gulyaev wave degenerates to the shear bulk wave. The ceramic material is poled in the x_3 direction determined by the right-hand rule from the x_1 and x_2 axes. The structure allows the following anti-plane motion [8]

$$u_1 = u_2 = 0 \ , \quad u_3 = u_3\left(x_1, x_2, t\right) \ , \quad \phi = \phi\left(x_1, x_2, t\right)$$

where u_1, u_2 and u_3 are the mechanical displacement components and ϕ the electric potential. The constitutive relations of 6 mm piezoelectric materials

that relate the stress components σ_{ij} and the electric displacement D_i to the mechanical displacement u_3 are given by Royer and Dieulesaint [9]

$$\sigma_{13} = c_{55}\frac{\partial u_3}{\partial x_1} + e_{15}\frac{\partial \phi}{\partial x_1}\ , \quad \sigma_{23} = c_{44}\frac{\partial u_3}{\partial x_2} + e_{24}\frac{\partial \phi}{\partial x_2} \tag{1}$$

$$D_1 = e_{15}\frac{\partial u_3}{\partial x_1} - \varepsilon_{11}\frac{\partial \phi}{\partial x_1}\ , \quad D_2 = e_{24}\frac{\partial u_3}{\partial x_2} - \varepsilon_{22}\frac{\partial \phi}{\partial x_2} \tag{2}$$

where (c_{44}, c_{55}), (e_{24}, e_{15}) and $(\varepsilon_{11}, \varepsilon_{22})$ are elastic, piezoelectric, and dielectric constants, respectively. Furthermore, the equation of motion and Gauss equation of piezoelectric materials without body force and free charge are

$$\frac{\partial \sigma_{31}}{\partial x_1} + \frac{\partial \sigma_{32}}{\partial x_2} = \rho_s \frac{\partial^2 u_3}{\partial t^2}\ , \quad \frac{\partial D_1}{\partial x_1} + \frac{\partial D_2}{\partial x_2} = 0 \tag{3}$$

where ρ_s is the mass density. By substituting Eq. (1) and Eq. (2) into Eq. (3), and using the macroscopic symmetry, the governing equations can be obtain by letting $c_{55} = c_{44}$, $e_{24} = e_{15}$, and $\varepsilon_{22} = \varepsilon_{11}$ in Eq. (3), i.e.

$$c_{44}\nabla^2 u_3 + e_{24}\nabla^2 \phi = \rho_s \frac{\partial^2 u_3}{\partial t^2} \tag{4}$$

$$e_{24}\nabla^2 u_3 - \varepsilon_{11}\nabla^2 \phi = 0 \tag{5}$$

where $\nabla^2 = \frac{\partial^2}{\partial x_1^2} + \frac{\partial^2}{\partial x_2^2}$ is the two dimensional Laplace operator.

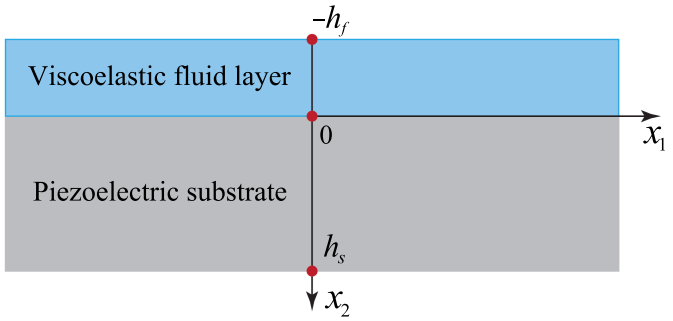

Figure 1: A finite-thickness piezoelectric substrate covered with a finite-thickness layer of viscoelastic fluid.

2.2. Viscoelastic fluid

The fluid occupying $-h_f < x_2 < 0$ is assumed to be viscoelastic and nonconductive. To describe the viscoelasticity of the fluid, the Maxwell and Kelvin-Voigt models are employed (see Figure 2). The Maxwell model introduces the viscoelastic response of the fluid at high frequencies and that of Kelvin-Voigt at low frequencies. The Maxwell model consists of a spring and a damper connected in series, and for the Kelvin-Voigt model, the spring and the damper are connected in parallel. The damper represents energy losses and is characterized by the viscosity η, whereas the spring represents the energy storage and is characterized by the elastic shear modulus μ. These two quantities are related through the relaxation time $\delta = \eta/\mu$, which is the characteristic time for the transition between viscous and elastic behavior [19]. Thus, suppose the motion of the fluid is induced only by wave propagation in the piezoelectric material and also propagates in the form of a harmonic wave. In regard to this problem, the inertial term in the Navier-Stokes equation can be omitted. Moreover, the pressure gradient can also be ignored since only shear deformation occurs during wave propagation [13]. In other words, the total stress in fluid is equal to the shear stress. Therefore, the governing equation for the viscoelastic fluid is simplified to the following

$$\rho_f \frac{\partial v_3}{\partial t} = \frac{\partial \tau_{13}}{\partial x_1} + \frac{\partial \tau_{23}}{\partial x_2} \tag{6}$$

where ρ_f is the density, v_3 is the velocity and (τ_{13}, τ_{23}) are the shear stress components. Thus, the constitutive equations which relate the shear stress tensor to velocity are

$$\tau_{13} + \delta \frac{\partial \tau_{13}}{\partial t} = \eta \frac{\partial v_3}{\partial x_1}\ , \quad \tau_{23} + \delta \frac{\partial \tau_{23}}{\partial t} = \eta \frac{\partial v_3}{\partial x_2} \tag{7}$$

$$\frac{\partial \tau_{13}}{\partial t} = \frac{\mu}{2} \frac{\partial v_3}{\partial x_1} + \eta \frac{\partial^2 v_3}{\partial t \partial x_1}\ , \quad \frac{\partial \tau_{23}}{\partial t} = \frac{\mu}{2} \frac{\partial v_3}{\partial x_2} + \eta \frac{\partial^2 v_3}{\partial t \partial x_2} \tag{8}$$

The relation (7) is suggested by Maxwell for the characterization of viscous fluids with elastic properties, and the relation (8) is proposed by Kelvin-Voigt for the description of elastic solids with viscous properties. Moreover, Eqs. (6)-(8) can be combined to give the following viscoelastic fluid equations

$$\nabla^2 v_3 - \frac{\rho_f}{\eta} \left(\frac{\partial v_3}{\partial t} + \delta \frac{\partial^2 v_3}{\partial t^2} \right) = 0 \tag{9}$$

$$\nabla^2 v_3 + 2\delta \frac{\partial}{\partial t} \nabla^2 v_3 - \frac{2\delta \rho_f}{\eta} \frac{\partial^2 v_3}{\partial t^2} = 0 \tag{10}$$

Equation (9) describes the fluid motion according to the Maxwell behavior and Eq. (10) to that of Kelvin-Voigt behavior. The solution of these equations and those of Eqs. (1) and (2) are to be substituted in the relevant boundary conditions.

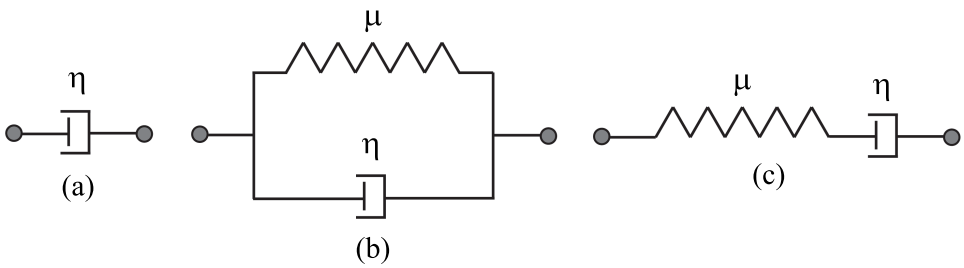

Figure 2: Schematic of (a) Newtonian (b) Kelvin-Voigt and (c) Maxwell models.

2.3. Boundary conditions

The solution of the Bleustein-Gulyaev wave propagation must satisfy the boundary conditions on the piezoelectric substrate and fluid, and the continuity conditions along the interface between the piezoelectric substrate and the fluid. At the interface $x_2 = 0$, the mechanical conditions are continuity of velocity and stress components, i.e.

$$v_3 = \frac{\partial u_3}{\partial t} \ , \ \tau_{23} = \sigma_{23} \quad \text{at} \quad x_2 = 0 \tag{11}$$

The surface of the fluid is open boundary. This requires

$$\tau_{23} = 0 \quad \text{at } x_2 = -h_f \tag{12}$$

The surface of the substrate is traction free and electrically open. This requires

$$\sigma_{23} = 0 \ , \ D_2 = 0 \quad \text{at } x_2 = h_s \tag{13}$$

Assume that the fluid is electrically insulated and its permittivity is much less than that of the piezoelectric substrate material. The electrical boundary conditions at the substrat-fluid interface can thus be classified into two cases

(i) an electrically open circuit (no density of charges) : $D_2(x_2 = 0) = 0$.

(ii) an electrically short circuit (matching to an external electric field) : $\phi(x_2 = 0) = 0$.

2.4. Solution of Bleustein-Gulyaev wave equations and dispersion relation

For this plane wave propagation problem in the x_1-direction, with displacement in x_3-direction only, the displacement component u_3, electric potential ϕ and velocity component v_3 can be assumed to take the following form

$$u_3 = U(x_2)\, e^{j(kx_1-\omega t)} \ , \ \phi = \Phi(x_2)\, e^{j(kx_1-\omega t)} \ , \ v_3 = V(x_2)\, e^{j(kx_1-\omega t)} \tag{14}$$

where k is the wavenumber along the propagation direction, ω is the angular frequency, and $U(x_2), \Phi(x_2)$ and $V(x_2)$ are the unknown functions of x_2. Bleustein-Gulyaev wave propagating in the piezoelectric substrate undergoes attenuation due to viscoelastic fluid, hence, the wavenumber becomes complex $k = k_r + jk_i$, its real part k_r describes the Bleustein-Gulyaev wave velocity, and its imaginary part k_i, is the Bleustein-Gulyaev wave attenuation induced by the viscoelastic fluid. After substitution of the expression (14) into Eqs. (4), (5), (9) and (10), the x_2 dependence can be expressed as

$$\begin{aligned} U(x_2) &= A_s e^{-\beta_s x_2} + B_s e^{\beta_s x_2} \\ \Phi(x_2) &= \frac{e_{24}}{\varepsilon_{11}} \left(A_s e^{-\beta_s x_2} + B_s e^{\beta_s x_2} \right) + C_s e^{-kx_2} + D_s e^{kx_2} \\ V(x_2) &= A_f e^{-\beta_f x_2} + B_f e^{\beta_f x_2} \end{aligned} \tag{15}$$

where A_s, B_s, C_s, D_s, A_f and B_f are arbitrary amplitudes and the wavenumbers β_s and β_f are given in the following form

$$\beta_s^2 = k^2 - \frac{\omega^2}{c_t^2} \quad , \quad \beta_f^2 = k^2 - \frac{j\omega\rho_f}{\eta^*}$$

Here, on the one hand we have defined the piezoelectrically stiffened elastic speed $c_t = \sqrt{\bar{c}_{44}/\rho_s}$, the piezoelectrically stiffened shear elastic coefficient $\bar{c}_{44} = c_{44}(1+\kappa^2)$ in the case of an electrically open circuit, and the electromechanical coupling factor $\kappa = e_{24}/\sqrt{c_{44}\varepsilon_{11}}$. Note that in the case of an electrically short circuit the piezoelectrically stiffened shear elastic coefficient thakes the following form $\bar{c}_{44} = c_{44}(1+\kappa^2/(1+\kappa^2))$. On the other hand, the complex dynamic viscosity η^* present in the wavenumber β_f can be defined according to the used viscoelastic fluid behavior as

$$\eta^* = \begin{cases} \dfrac{\eta}{1-j\omega\delta} & \text{Maxwell model} \\ \eta - \dfrac{\eta}{2j\omega\delta} & \text{Kelvin-Voigt model} \end{cases} \tag{16}$$

The shear stress component and electric displacement that will be used in boundary conditions are given by

$$\begin{aligned} D_2 &= k\varepsilon_{11}\left(C_s e^{-kx_2} - D_s e^{kx_2}\right) e^{j(kx_1-\omega t)} \\ \sigma_{23} &= \left[\beta_s \bar{c}_{44}\left(B_s e^{\beta_s x_2} - A_s e^{-\beta_s x_2}\right) - k e_{24}\left(C_s e^{-kx_2} - D_s e^{kx_2}\right)\right] e^{j(kx_1-\omega t)} \\ \tau_{23} &= \beta_f \eta^* \left(B_f e^{\beta_f x_2} - A_f e^{-\beta_f x_2}\right) e^{j(kx_1-\omega t)} \end{aligned} \tag{17}$$

Substitution of the Eqs. (15) and (17) into the boundary and continuity conditions (11)-(13) yields a system of six linear algebraic equations in six undetermined amplitudes. For nontrivial solutions of the undetermined amplitudes to exist, the determinant of this system has to equal zero, which leads to the following dispersion relation of the Bleustein-Gulyaev waves in the case of an electrically short circuit :

$$\bar{c}_{44}\beta_s \tanh\left(\beta_s h_s\right) - j\omega\eta^*\beta_f \tanh\left(\beta_f h_f\right) - \frac{e_{24}^2}{\varepsilon_{11}} k \tanh\left(k h_s\right) = 0 \tag{18}$$

and in the case of an electrically open circuit :

$$\bar{c}_{44}\beta_s \tanh\left(\beta_s h_s\right) - j\omega\eta^*\beta_f \tanh\left(\beta_f h_f\right) = 0 \tag{19}$$

Since these relations contains k, ω, as well as all material and geometrical parameters of the viscoelastic fluid and piezoelectric substrate, Eqs. (18) and (19) represent the explicit complex dispersion relation of Bleustein-Gulyaev waves propagating in a piezoelectric substrate loaded with a viscoelastic fluid. Eqs. (18) and (19) were solved using Mathematica software. Once the wavenumber is obtained, the phase velocity is calculated by $v_p = \omega/k_r$. While the imaginary part of wavenumber k_i represents the attenuation per unit length in the propagation direction. Furthermore, the critical term $\delta\omega$ present in the complex dynamic viscosity η^* depends both on δ and ω. The three following regimes may be highlighted in the case of :

- Maxwell fluid: (i) For $\delta\omega \ll 1$ the oscillation time $(= 1/\omega)$ is greater than the relaxation time and, the liquid exhibits purely Newtonian behavior. (ii) For $\delta\omega \gg 1$ the oscillation time is smaller than the relaxation time and, the liquid exhibits viscoelastic behavior. (iii) For $\delta\omega = 1$ the transition from Newtonian to Maxwell regime takes place.

- Kelvin-Voigt fluid: (i) For $\delta\omega \ll 1$ the oscillation time is greater than the relaxation time and, the liquid exhibits viscoelastic behavior. (ii) For $\delta\omega \gg 1$ the oscillation time is smaller than the relaxation time and, the liquid exhibits purely Newtonian behavior. (iii) For $\delta\omega = 1$ the transition from Newtonian to Kelvin-Voigt fluid regime takes place.

2.4.1. Some particular cases

For the special case when $h_s \to \infty$ (piezoelectric substrate half-space), we can separately degenerate Eqs. (18) and (19) into the following

$$\bar{c}_{44}\beta_s - j\omega\eta^*\beta_f \tanh(\beta_f h_f) - \frac{e_{24}^2}{\varepsilon_{11}}k = 0 \tag{20}$$

$$\bar{c}_{44}\beta_s - j\omega\eta^*\beta_f \tanh(\beta_f h_f) = 0 \tag{21}$$

In the case of a Newtonian fluid ($\eta^* = \eta$), Eqs. (20) and (21) are exactly the same as those obtained previously by Qian *et al.* [14]. When $h_f \to \infty$ (fluid half-space), the Eqs. (20) and (21) become

$$\bar{c}_{44}\beta_s - j\omega\eta\beta_f - \frac{e_{24}^2}{\varepsilon_{11}}k = 0 \tag{22}$$

$$\bar{c}_{44}\beta_s - j\omega\eta\beta_f = 0 \tag{23}$$

which were previously obtained by Guo and Sun [13].

3. Numerical results and discussion

The material properties given in Table 1 for the PZT-5H piezoelectric ceramic substrate [14, 20], and in Table 2 for viscoelastic fluid [21] are considered. In this work, numerical calculation is performed in the glycerol concentrations range from 15.4% to 88.0%. In addition, the Bleustein-Gulyaev wave velocities in the PZT-5H piezoelectric ceramic substrate c_t are obtained from the work of Bleustein [8].

The Bleustein-Gulyaev surface waves are defined in plates of an infinite thickness and therefore have only one fundamental mode ($n = 1$). The high order plate modes ($n = 2, 3, 4, ...$) occur in piezoelectric plates of finite thickness. Figure 3 shows the Bleustein-Gulyaev wave ($n = 1$) and higher order SH plate waves versus substrate thickness. It is seen that when the substrate is very thin, the first mode velocity tends to the substrate shear wave velocity for a short circuit ($c_{sc} = c_t = 2039.445$, see Table 1). When

	c_{44} (GPa)	ρ_s (kg/m^3)	e_{24} (C/m^2)	ε_{11} (F/m)	c_t (m/s)
Short circuit	23	7500	17	$227 \cdot 10^{-10}$	2039.445
Open circuit	23	7500	17	$227 \cdot 10^{-10}$	2182.697

Table 1: Material parameters used for PZT-5H piezoelectric ceramic substrate.

χ (%)	η (mPa $\cdot$ s)	ρ_f (kg/m^3)	δ (ps)
15.4	1.4	1017	28
25.6	1.7	1029	38
32.9	2.7	1038	54
37.3	3.1	1044	62
42.3	3.8	1050	76
46.7	4.6	1055	92
52.2	5.9	1062	118
62.1	10.2	1075	204
72.0	21.9	1087	438
75.9	33.2	1093	664
80.0	49.5	1098	990
84.0	81.8	1104	1636
88.0	128.1	1109	2562

Table 2: Material parameters used for water-glycerol mixtures. χ is the concentration of glycerol in water and ps defines the picosecond.

increasing the layer thickness, the velocity of the higher order modes assymptotically reaches the first mode velocity. Thus, in this work, the attention is focused on the properties of the fundamental mode. In addition, the first mode phase velocity in the substrate was calculated in Table 3 in the case of a short and an open circuits for both Newtonian and viscoelastic fluids. The numerical calculations are performed for three Glycerol concentrations $(15.4\%, 52.2\%, 88\%)$ and two frequencies (100 MHz, 200 MHz). In each case, it is shown that the velocity varies little with glycerol concentration and with frequency and remains very close to the substrate shear wave velocity. Note that similar behavior was observed by [13, 14].

The water glycerol mixture behaves like a viscoelastic solid for high con-

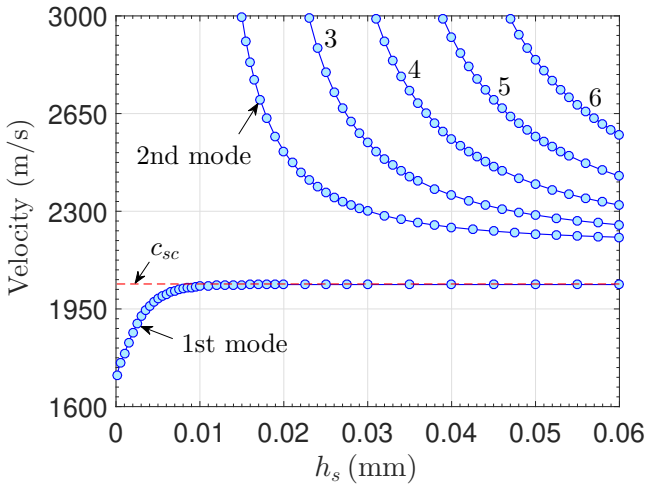

Figure 3: Phase velocity versus the piezoelectric substrate thickness in the case of "short" circuit and Maxwell model with $\chi = 37.3\,\%$, $h_f = 0.05\,\text{mm}$ and $f = 200\,\text{MHz}$.

Short circuit	Newtonian		Maxwell		Kelvin-Voigt	
χ (%)	100 MHz	200 MHz	100 MHz	200 MHz	100 MHz	200 MHz
15.4	2038.441	2038.026	2038.450	2038.052	2039.428	2039.291
52.2	2037.341	2036.471	2037.424	2036.718	2038.993	2038.435
88.0	2029.553	2025.626	2036.828	2038.049	2031.120	2026.843
Open circuit	Newtonian		Maxwell		Kelvin-Voigt	
χ (%)	100 MHz	200 MHz	100 MHz	200 MHz	100 MHz	200 MHz
15.4	2182.648	2182.663	2182.649	2182.664	2182.726	2182.725
52.2	2182.595	2182.626	2182.599	2182.633	2182.706	2182.708
88.0	2182.228	2182.466	2182.620	2182.731	2182.341	2182.544

Table 3: First mode phase velocity with $h_s = 0.1\,\text{mm}$ and $h_f = 0.05\,\text{mm}$.

centration of glycerol. Therefore, the Kelvin-Voigt model is suitable for high viscosity. Otherwise, the Maxwell model can be used to calculate the atten-

uation for low glycerol concentration.

3.1. Influence of the glycerol mass fraction

In this paragraph, we investigate how the phase velocity and attenuation vary with the glycerol mass fraction (i.e., shear viscosity) for a short and for an open circuits in both Newtonian and viscoelastic fluids. In Figures 4 and 5, increasing the glycerol mass fraction, Newtonian and Kelvin-Voigt models predicted a monotonically decreasing relationship between the vibrations responses and the glycerol mass fraction. However, Maxwell model highlighted a non-monotonically behavior wich manifested the intrinsic viscoelastic properties of fluid. The elastic effects are significant for glycerol concentration greater than 52% (100 MHz) and 37% (200 MHz). For glycerol concentration values less than theses critical values, the elasticity can be neglected and the behavior is Newtonian. This is due to the time constant value less than 118 ps and 62 ps corresponding to $\delta\omega$ less than 0.0741 and 0.0779 negligible compared to 1. Otherwise, as expected, the gap between the Newtonian and Kelvin-Voigt models decreases with increasing viscosity. Thus, the convergence of these two models is stronger in the case of an open circuit at high frequencies. In conclusion, the water glycerol mixture behaves like a viscoelastic solid for high concentration of glycerol. Therefore, the Kelvin-Voigt model is suitable for high viscosity. Otherwise, the Maxwell model can be used to calculate the attenuation for low glycerol concentration.

3.2. Substrate thickness effect

Figures 6 and 7 illustrate the influence of substrate thickness on the attenuation for two glycerol mixtures and different frequencies values. These figures highlight that the attenuation decresases rapidly for low substrate thickness and then reaches a plateau region. The substrate thickness allowing access to the plateau region are equal to 0.02 mm (short circuit) and 0.03 mm (open circuit). Theses values are much lower than the typical thickness (10 mm) used in design of Bleustein-Gulyaev wave sensors [3, 11]. Figures 6 and 7 also show that the attenuation incresases with frequency and glycerol mass fraction. Moreover, the attenuation values in the case of the short circuit are stronger than those in the open circuit case. Otherwise, the numerical results obtained with the Maxwell and Newtonian models converge for low frequencies (see Figure 6). The similar phenomenon appears on the Figure 7 for Kelvin-Voigt fluid but the difference between the two models is less significant.

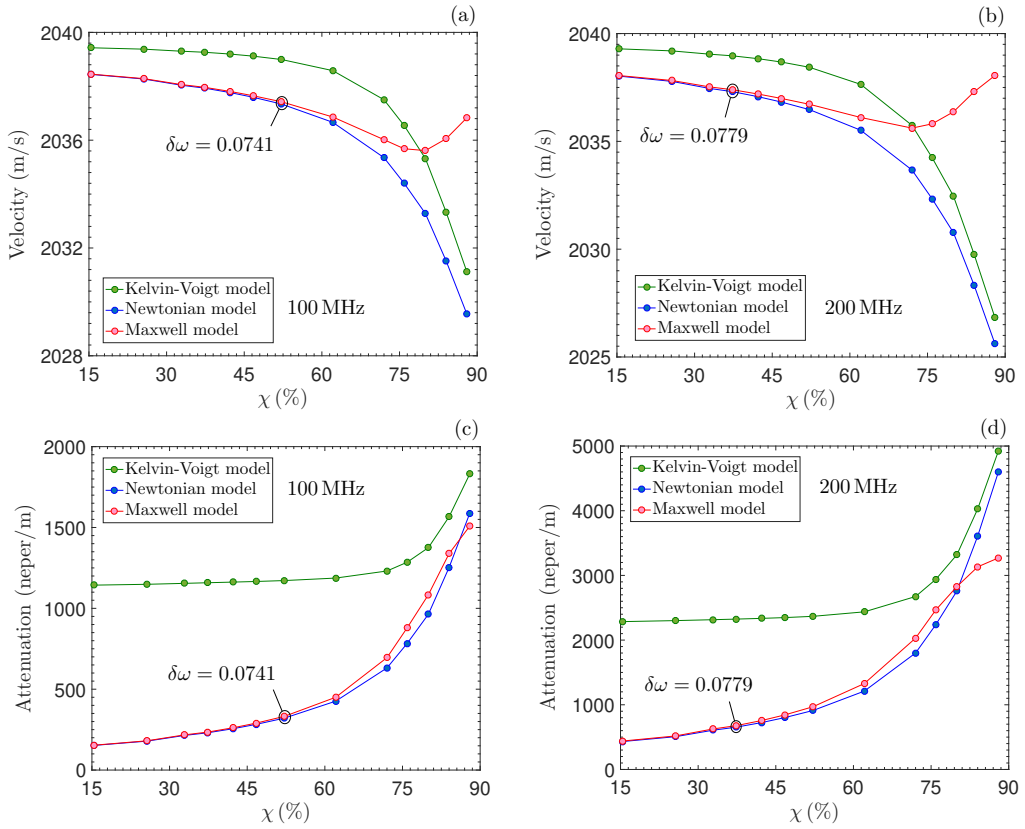

Figure 4: First mode velocity and attenuation versus the glycerol mass fraction in the case of "short" circuit with $h_s = 0.1\,\text{mm}$ and $h_f = 0.05\,\text{mm}$.

3.3. Fluid thickness effect

The wave attenuation with respect to the fluid thickness is shown in Figures 8 and 9. It can be seen that the attenuation increases with fluid thickness, then reaches a maximum and keeps a constant value. The attenuation increases with frequency and glycerol concentration. Comparing these Figures, we can see that attenuation in the short ciruit condition is much larger than for open circuit. This is coherent with the fact that the metallization decreases the penetration depth in the substrate [14]. Hence, in short circuit condition the wave energy is confined in the vicinity of the surface. Consequently, the velocity and attenuation are very sensitive to fluid loading. Otherwise, it is highlighted that the results obtained with the Maxwell and Newtonian models converge for low frequencies. The same phenomenon (far

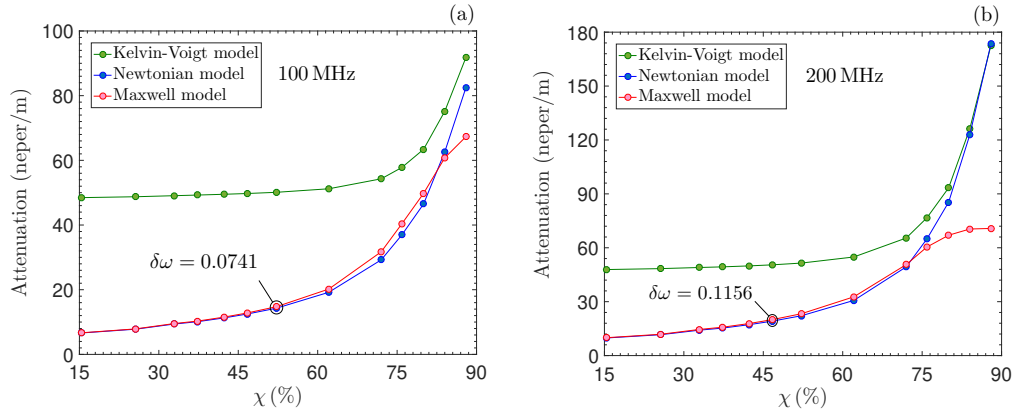

Figure 5: First mode attenuation versus the glycerol mass fraction in the case of "open" circuit with $h_s = 0.1\,\text{mm}$ and $h_f = 0.05\,\text{mm}$.

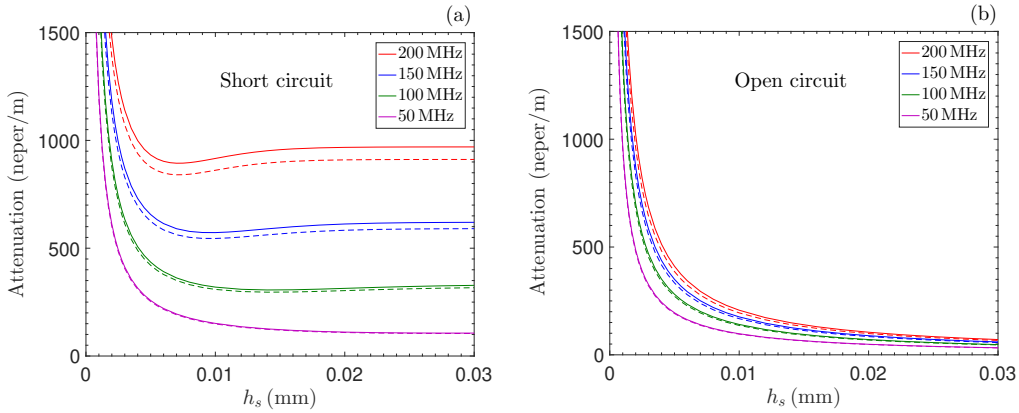

Figure 6: First mode attenuation versus piezoelectric substrate thickness for a glycerol mass fraction of $\chi = 52.2\%$ with $h_f = 0.05\,\text{mm}$. Maxwell fluid (solid lines); Newtonian fluid (dashed lines).

less significant) is observed in the case of short circuit. The gap between the Kelvin-Voigt and Newtonian curves decreases with frequency. The opposite behavior is shown for open circuit, the Kelvin-Voigt curves join the Newton ones for high frequencies.

3.4. Frequency effect

The frequency effect on the attenuation is depicted in Figures 10 and 11 for a short and for an open circuits. The attenuation due to Newtonian

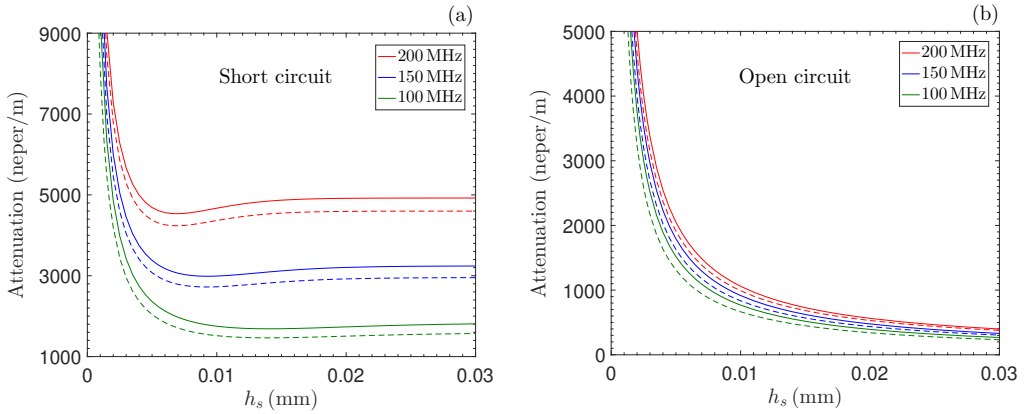

Figure 7: First mode attenuation versus piezoelectric substrate thickness for a glycerol mass fraction of $\chi = 88.0\%$ with $h_f = 0.05\,\text{mm}$. Kelvin-Voigt fluid (solid lines); Newtonian fluid (dashed lines).

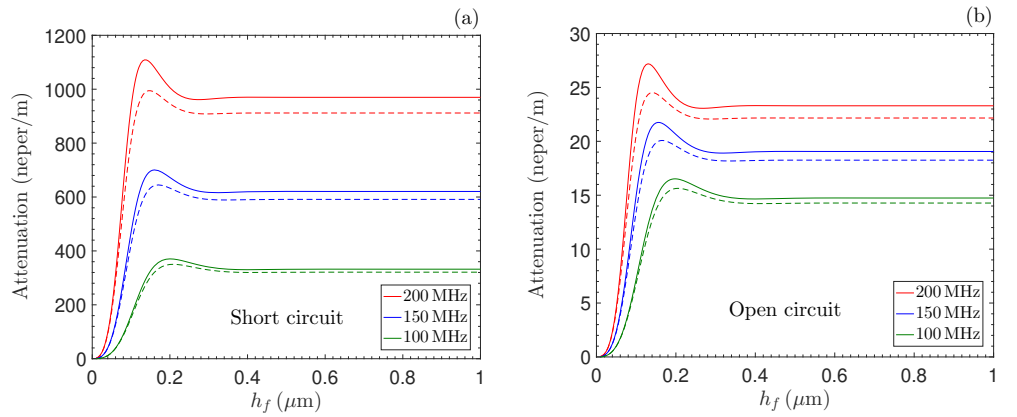

Figure 8: First mode attenuation versus fluid thickness for a glycerol mass fraction of $\chi = 52.2\%$ with $h_s = 0.1\,\text{mm}$. Maxwell fluid (solid lines); Newtonian fluid (dashed lines).

model increases with the frequency and is much larger for short circuit condition. It is seen that the attenuation values obtained with the Maxwell model converge towards those obtained with the Newtonian model for low frequencies. Otherwise, Figure 11 (open circuit) highlights another phenomenon, the Kelvin-Voigt and Newtonian curves diverge at low frequencies and converge for high frequencies. It is seen from Figure 11(b) that the difference between Kelvin-Voigt attenuation values is negligible for high glycerol concentration (88%) and high frequency (200 MHz). This last result can be explained by

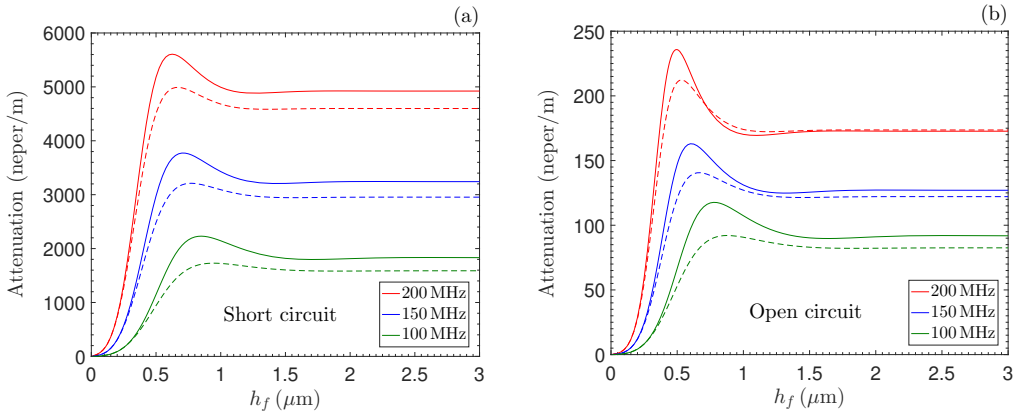

Figure 9: First mode attenuation versus fluid thickness for a glycerol mass fraction of $\chi = 88.0\%$ with $h_s = 0.1\,\text{mm}$. Kelvin-Voigt fluid (solid lines); Newtonian fluid (dashed lines).

a negligible difference between Kelvin-Voigt and Newtonian viscosities for high glycerol concentration and high frequency.

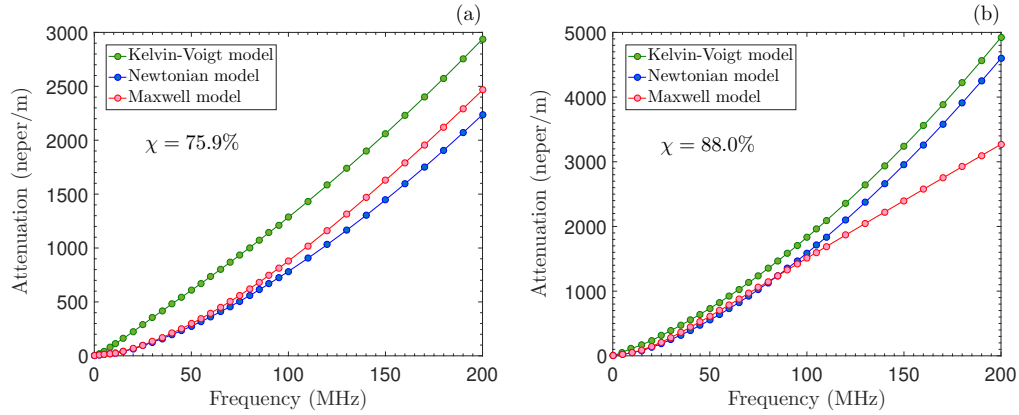

Figure 10: First mode attenuation versus frequency in the case of a short circuit with $h_s = 0.1\,\text{mm}$ and $h_f = 0.05\,\text{mm}$.

4. Conclusion

Propagation of Bleustein-Gulyaev waves in a finite-thickness piezoelectric ceramic substrate loaded with a viscoelastic fluid is investigated using a new original approach based on the exact theory. The Maxwell and Kelvin-Voigt

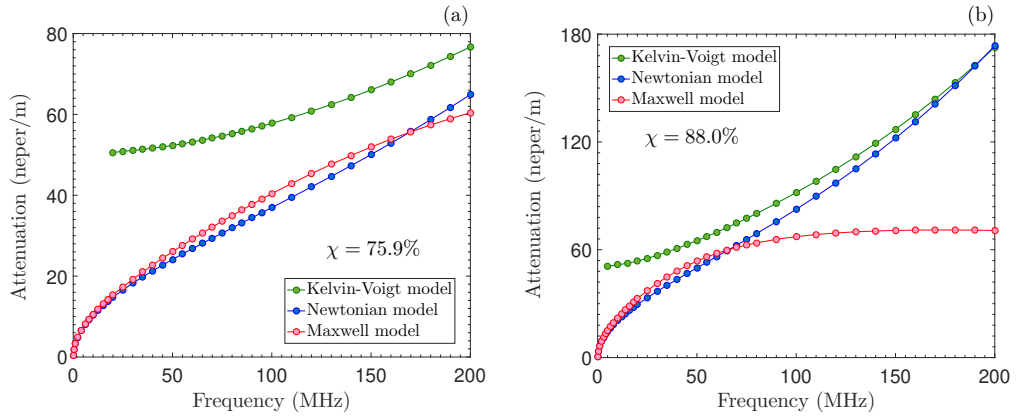

Figure 11: First mode attenuation versus frequency in the case of an open circuit with $h_s = 0.1\,\text{mm}$ and $h_f = 0.05\,\text{mm}$.

models were employed to describe the viscoelasticity of the fluid. The explicit dispersion equations for both open circuit and short circuit were given. Those equations were used to study the influence of the substrate thickness, fluid thickness, glycerol concentration and frequency on the wave propagation. It was highlighted that the electrically short circuit is more sensitive than the open circuit to surrounding disturbance. This is due to the confinement of the wave in the vicinity of the surface. It is also shown that the Maxwell and Newtonian curves converge for low frequency or low glycerol concentration. Furthermore, the gap between the Kelvin-Voigt and Newton curves decreases when frequency or glycerol concentration increases. Finally the new dispersion equations proposed in this work can be used to develop and design Bleustein-Gulyaev sensors waves loaded with a viscoelastic fluid.

References

[1] J. O. Kim. The effect of a viscous fluid on Love waves in a layered medium, *The Journal of the Acoustical Society of America* **91**(6), 3099 (1992).

[2] J. Du, G. L. Harding, J. A. Ogilvy, P. R. Dencher and M. Lake. A study of Love-wave acoustic sensors, *Sensors and Actuators A: Physical* **56**(3), 211–219 (1996).

[3] P. Kielczynski, M. Szalewski and A. Balcerzak. Effect of a viscous liquid

loading on Love wave propagation, *International Journal of Solids and Structures* **49**(17), 2314–2319 (2012).

[4] A. El Baroudi. Influence of poroelasticity of the surface layer on the love wave propagation, *Journal of Applied Mechanics* **85**(5), 051002 (2018).

[5] A. El Baroudi and J. Y. Le Pommellec. Viscoelastic fluid effect on the surface wave propagation, *Sensors and Actuators A: Physical* **291**(1), 188–195 (2019).

[6] A. El Baroudi and J. Y. Le Pommellec. Surface wave in a Maxwell liquid-saturated poroelastic layer, *Applied Acoustics* **159**, 107076 (2020).

[7] H. F. Tiersten. Wave Propagation in an Infinite Piezoelectric Plate, *The Journal of the Acoustical Society of America* **35**(2) (1963).

[8] J. L. Bleustein. A new surface wave in piezoelectric materials, *Applied Physics Letters* **13**(12) (1968).

[9] D. Royer and E. Dieulesaint. Elastic Waves in Solids: Free and Guided Propagation, Springer, New York (2000).

[10] C. Zhang, J. J. Caron and J. F. Vetelino. The Bleustein-Gulyaev wave for liquid sensing applications, *Sensors and Actuators B: Chemical* **76**(1-3), 64–68 (2001).

[11] P. Kielczynski, W. Pajewski, M. Szalewski, and A. Balcerzak. Measurement of the shear storage modulus and viscosity of liquids using the Bleustein-Gulyaev wave, *Review of Scientific Instruments* **75**, 2362 (2004).

[12] P. Kielczynski, M. Szalewski, R. M. Siegoczynski and A. J. Rostocki. New ultrasonic Bleustein-Gulyaev wave method for measuring the viscosity of liquids at high pressure, *Review of Scientific Instruments* **79**, 026109 (2008).

[13] F. L. Guo and R. Sun. Propagation of Bleustein-Gulyaev wave in 6 mm piezoelectric materials loaded with viscous liquid, *International Journal of Solids and Structures* **45**(13), 3699–3710 (2008).

[14] Z. H. Qian, F. Jin, P. Li and S. Hirose. Bleustein-Gulyaev waves in 6mm piezoelectric materials loaded with a viscous liquid layer of finite thickness, *International Journal of Solids and Structures* **47**, 3513–3518 (2010).

[15] F. L. Guo, G. Q. Wang and G. A. Rogerson. Inverse determination of liquid viscosity by means of Bleustein-Gulyaev wave, *International Journal of Solids and Structures* **49**(15-16), 2115–2120 (2012).

[16] P. Kielczynski, M. Szalewski, A. Balcerzaka, A. Malanowski, R. M. Siegoczynski and S. Ptasznik. Investigation of high-pressure phase transitions in DAG (diacylglycerol) oil using the Bleustein-Gulyaev ultrasonic wave method, *Food Research International* **49**(1), 60–64 (2012).

[17] P. Kielczynski, S. Ptasznik, M. Szalewski, A. Balcerzaka, K. Wieja and A. J. Rostocki. Thermophysical properties of rapeseed oil methyl esters (RME) at high pressures and various temperatures evaluated by ultrasonic methods, *Biomass and Bioenergy* **107**, 113–121 (2017).

[18] P. Kielczynski, M. Szalewski, A. Balcerzaka, K. Wieja, A. J. Rostocki and S. Ptasznik. Investigation of high-pressure phase transitions in biofuels by means of ultrasonic methods, IEEE International Ultrasonics Symposium (2016).

[19] D. D. Joseph. Fluid dynamics of viscoelastic liquids. Springer (1990).

[20] H. Y. Fang, J. S. Yang and Q. Jiang. Rotation-perturbed surface acoustic waves propagating in piezoelectric crystals, *International Journal of Solids and Structures* **37**(36), 4933-4947 (2000).

[21] K. Mitsakakis, A. Tsortos, J. Kondoh, E. Gizeli, Parametric study of SH-SAW device response to various types of surface perturbations, *Sensors and Actuators B: Chemical* **138**(2), 408–416 (2009).